New Journal of Physics
The open access journal for physics

Thermal versus entanglement entropy: a measurement protocol for fermionic atoms with a quantum gas microscope

Hannes Pichler[1,2,4], Lars Bonnes[1], Andrew J Daley[3], Andreas M Läuchli[1] and Peter Zoller[1,2]

[1] Institute for Theoretical Physics, University of Innsbruck, A-6020 Innsbruck, Austria
[2] Institute for Quantum Optics and Quantum Information of the Austrian Academy of Sciences, A-6020 Innsbruck, Austria
[3] Department of Physics and Astronomy, University of Pittsburgh, Pittsburgh, PA 15260, USA
E-mail: hannes.pichler@uibk.ac.at

New Journal of Physics **15** (2013) 063003 (17pp)
Received 6 February 2013
Published 6 June 2013
Online at http://www.njp.org/
doi:10.1088/1367-2630/15/6/063003

Abstract. We show how to measure the order-two Renyi entropy of many-body states of spinful fermionic atoms in an optical lattice in equilibrium and non-equilibrium situations. The proposed scheme relies on the possibility to produce and couple two copies of the state under investigation, and to measure the occupation number in a site- and spin-resolved manner, e.g. with a quantum gas microscope. Such a protocol opens the possibility to measure entanglement and test a number of theoretical predictions, such as area laws and their corrections. As an illustration we discuss the interplay between thermal and entanglement entropy for a one dimensional Fermi–Hubbard model at finite temperature, and its possible measurement in an experiment using the present scheme.

[4] Author to whom any correspondence should be addressed.

Contents

1. Introduction

Quantum degenerate gases, and ultracold atoms in optical lattices in particular, provide a unique framework to study quantum many-body physics [1–4]. This refers first of all to the possibility of controlling many-body dynamics via external fields, thus allowing one to effectively engineer a wide class of interesting many-particle Hamiltonians, including those for strongly correlated systems [5–8]. Furthermore, a plethora of new measurement tools are available in atomic setups based on probing atoms with laser light, providing access to physical observables of many-body dynamics, in a way which is unparalleled in a condensed matter context. An outstanding example is the recent development of a 'quantum gas microscope' for atoms in optical lattices, which allows single-atom detection and imaging with resolution of the lattice spacing in single-shot measurements [9, 10]. Given these unique and novel tools the challenge is now to identify new atomic measurement protocols that allow access to new many-particle observables of interest. Below we describe such a protocol, which allows the direct measurement of the Renyi entropies, quantifying uncertainty due to *thermal fluctuations and due to entanglement*, of (spinful) *fermionic* atoms in optical lattices for both equilibrium and non-equilibrium situations. The protocol consists of preparing two identical copies of the many-body systems in one-dimensional (1D) or two-dimensional (2D) optical lattices, performing simple single particle operations that are readily implemented in optical lattices, followed by a read out with the quantum gas microscope. While in recent work [11] we have discussed such a protocol for bosonic atoms, the fermionic case requires rather different arguments resulting in a different translation table to interpret the measurement results, although—quite remarkably—the basic procedure parallels the case of bosons.

Direct measurement of thermal and entanglement entropy in atomic gases brings fundamental concepts, which so far have been discussed exclusively in a theoretical context, to the laboratory. Examples include the area law scaling that lies at the heart of the success of matrix product states methods [12] and logarithmic corrections in critical systems that

allow us access to properties of the underlying conformal field theory (CFT) [13, 14]. Also, the ability to explore higher dimensions is invaluable as the theoretical understanding of the corrections to the area law is less advanced and has sparked a lot of recent interest in the theory community [15–22]. Other exciting applications include the possibility to detect topological order [23, 24] or to monitor the dynamic generation of entanglement in quantum quenches [25–28]—which are also relevant to questions concerning thermalization in closed quantum systems [29–31]—as already implemented in cold-atom experiments [32]. An important question in this context will be to ask which amount of the entropy is due to entanglement and what contribution is thermal entropy. This leads into the question as to whether it is possible to access the quantum entangled regime in current experimental setups, at least for small systems.

To address the latter questions, we use quantum Monte Carlo (QMC) calculations to directly access the finite-temperature Renyi entropies for spinful fermions, described by a Hubbard model in one dimension. By comparing the finite-T results to ground state density matrix renormalization group (DMRG) calculations, we study the crossover between regimes dominated by quantum entanglement and regimes dominated by thermal entropy for realistic system parameters [33]. These simulation results allow us to give a critical assessment of when such a measurement could realistically be implemented by addressing the question of limitations of the measurement protocol. In particular, the exponential scaling of the number of single measurements with the entropy in the system sets the boundary in term of temperatures and system sizes, for what will be accessible under realistic circumstances.

2. Measurement protocol for Renyi entropies of fermionic atoms

We consider a many-body system represented by fermionic atoms in an optical lattice. The state of the system at a given time t is described by a density operator ρ. In the following discussion we leave the specific form of the state open. It can represent a pure state, $\rho = |\psi\rangle\langle\psi|$, such as the ground state of a Hamiltonian, a thermal state, or any other (mixed) non-equilibrium state of the fermionic atoms. Our goal is to develop a protocol to measure Renyi entropies both for the total system and for subsystems. For the total system the Renyi entropy of order two is defined by $S_2(\rho) = -\log \mathrm{Tr}\{\rho^2\}$, and thus is given in terms of the purity of the density operator $P_2(\rho) = \mathrm{Tr}\{\rho^2\}$. For a subsystem $\mathcal{R}$ we define a reduced density operator $\rho_\mathcal{R} = \mathrm{Tr}_{\neq\mathcal{R}}\{\rho\}$, and a corresponding Renyi entropy as $S_2(\rho_\mathcal{R}) = -\log \mathrm{Tr}\,\{\rho_\mathcal{R}^2\}$. The knowledge of both $S_2(\rho)$ and $S_2(\rho_\mathcal{R})$, allows one to quantify the entanglement of the subsystem $\mathcal{R}$ with the rest [34, 35]. While, as emphasized above, the following discussion is valid for any quantum state, specific scenarios of experimental interest include monitoring state purity and entanglement entropies in quench dynamics as a function of time, or thermal versus entanglement entropy in thermodynamic equilibrium situations.

The Renyi entropy and the purity are nonlinear functionals of the quantum state and thus not directly observable. However, the purity can be directly obtained by measuring several copies of the same state [36]. It can be expressed as the expectation value of the *swap operator* V_2 on a system that is prepared in two identical copies in the same quantum state ρ, that is, $\mathrm{Tr}\{\rho^2\} = \mathrm{Tr}\{V_2\rho\otimes\rho\} \equiv \langle V_2\rangle$, where the swap operator is defined as $V_2|\psi_1\rangle\otimes|\psi_2\rangle = |\psi_2\rangle\otimes|\psi_1\rangle$. Similarly, the purity of the reduced density operator of a subsystem $\mathcal{R}$ is given by the expectation value of the operator $V_2^\mathcal{R}$ that swaps the quantum states just in the part $\mathcal{R}$, that is $\mathrm{Tr}\{\rho_\mathcal{R}^2\} = \mathrm{Tr}\{V_2^\mathcal{R}\rho\otimes\rho\} \equiv \langle V_2^\mathcal{R}\rangle$. A measurement of the Renyi entropies $S_2(\rho)$ and $S_2(\rho_\mathcal{R})$

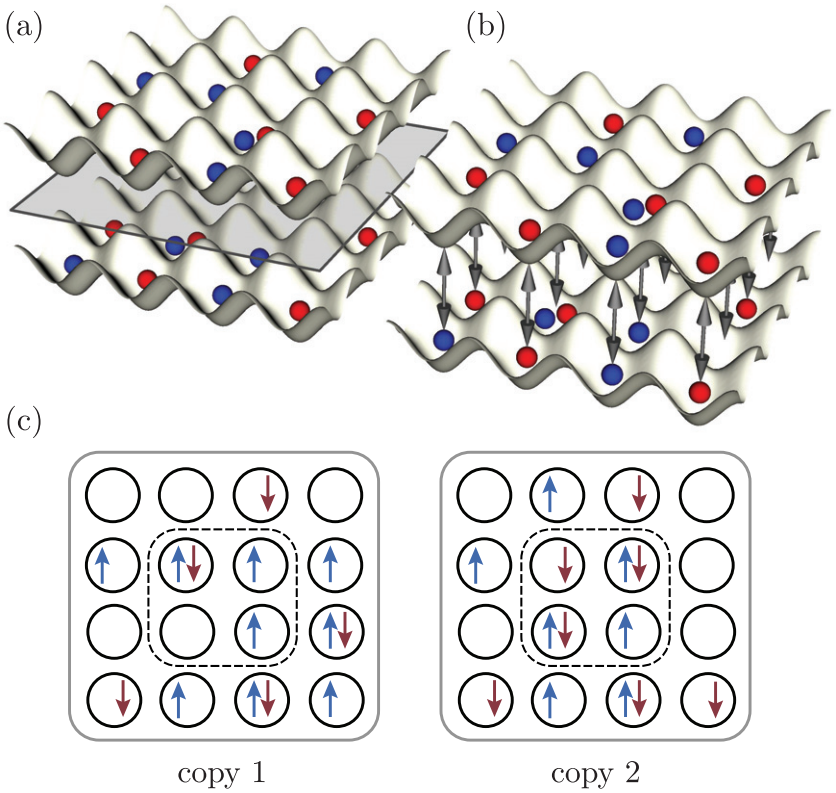

Figure 1. The three steps in the measurement protocol of second Renyi entropy for spinful fermions in a 2D optical lattice. (a) First, two copies of the many-body state are produced. (b) Then the barrier between the copies is lowered such that atoms can tunnel from each mode to its copy to realize a beam splitter operation between the copies (see equation (2)). (c) Finally, the fermion number is measured site- and spin-resolved in both copies with a quantum microscope. Here we show a typical outcome of a single measurement run, where on each site one finds either no atom, an atom with spin up, an atom with spin down or both spins on one site. In this example, according to table 1 the measurement outcome for the swap operator on the whole system is +1, while the result for the reduced set of modes that are enclosed by the dashed line is −1. Simultaneously one also obtains measurement results for all other subsets. For example the outcome for the swap operator on the spin up modes is −1.

of fermionic atoms in optical lattices thus reduces to (i) the ability to prepare two identical copies of the atomic system, and (ii) the development of a protocol to measure $\langle V_2 \rangle$ and $\langle V_2^{\mathcal{R}} \rangle$ by simple operations and read out in an optical lattice on the two copies, in a way that can be readily implemented with high fidelity in present experiments. While the first aspect is primarily an experimental question, we will focus in the following on the protocol to realize the measurement of the swap operation (ii) and interpretation of measurement results of a quantum gas microscope to determine $\langle V_2 \rangle$ and $\langle V_2^{\mathcal{R}} \rangle$. We comment on the assumption of identical copies (i) at the end of this section.

To be more specific, we consider spin-1/2 fermions in an optical lattice, in a setup illustrated for two 2D lattices representing the two copies in figure 1. We define a basis of

Fock states for the two copies of the system

$$|\mathbf{n}, \mathbf{m}\rangle \equiv \prod_{(i,\sigma)} (a^\dagger_{i,\sigma})^{n_{i,\sigma}} \prod_{(j,\sigma)} (b^\dagger_{j,\sigma})^{m_{j,\sigma}} |\mathrm{vac}\rangle, \tag{1}$$

where $a^\dagger_{i,\sigma}$ and $b^\dagger_{i,\sigma}$ denote the creation operations for fermionic atoms on lattice site i and spin $\sigma = \pm 1/2$ in the first and second system (copy), respectively, and where the $\mathbf{n} = \{n_{1,\uparrow}, n_{1,\downarrow}, n_{2,\uparrow}, \ldots\}$ and $\mathbf{m} = \{m_{1,\uparrow}, m_{1,\downarrow}, m_{2,\uparrow}, \ldots\}$ are the occupation numbers of the two systems. The swap operator V_2 acts on these states as $V_2|\mathbf{n}, \mathbf{m}\rangle = |\mathbf{m}, \mathbf{n}\rangle$, which interchanges the configurations $\mathbf{n}$ and $\mathbf{m}$. For bosons this swap operation amounts to the interchange $a^\dagger_{i,\sigma} \leftrightarrow b^\dagger_{i,\sigma}$. Daley *et al* [11] have shown that a measurement of this is readily implemented in an optical lattice by turning on tunneling between corresponding lattice sites of the two copies, and reading out lattice occupation of the first copy (modulo 2) with the quantum gas microscope. However, for fermions applying V_2 is *not* equivalent to exchanging $a^\dagger_{i,\sigma} \leftrightarrow b^\dagger_{i,\sigma}$, since there is an ordering problem, i.e. one must keep track of the fermionic signs. In the following we will present this protocol for fermions. We will present our results first in the form of an experimental *recipe* in section 2.1, and give the formal proof in section 2.2 and appendix A. In section 2.3 will analyze limitations and scaling of errors in these measurements.

2.1. *Experimental protocol to measure* $\mathrm{Tr}\{\rho^2_{\mathcal{R}}\} = \mathrm{Tr}\{\mathrm{V}^{\mathcal{R}}_2 \rho \otimes \rho\}$

The expectation value of $V_2^{\mathcal{R}}$ is obtained by averaging over a series of single measurements, where each single measurement proceeds in three steps as illustrated in figure 1.

(i) Initially two identical copies of the same (non-) equilibrium state are prepared [37]. With optical lattices this can be performed in two parallel 1D tubes or two neighboring 2D planes that are completely decoupled (cf figure 1(a)).

(ii) At a given time t the lattice depth within each copy is suddenly ramped up to freeze the atomic configuration by suppressing tunneling (atomic limit). Simultaneously, all interactions (e.g. between different spins) are turned off, e.g. by using magnetic or optical Feshbach resonances [38, 39]. Alternatively the protocol can be executed on a timescale where the effects of interactions are negligible. Note that during this step the entanglement and the overall entropy does not change.
We then lower the barrier between the two copies to allow tunneling between each site and its copy with an amplitude J_{ab} for a fixed time $\tau_{ab} = \pi/(4J_{ab})$ (cf figure 1(b)). This can be accomplished with the use of an optical superlattice [40]. With this operation we implement the beam splitter U_2 that maps

$$U_2 : a_{i,\sigma} \to \frac{1}{\sqrt{2}}(a_{i,\sigma} + b_{i,\sigma});\ b_{i,\sigma} \to \frac{1}{\sqrt{2}}(b_{i,\sigma} - a_{i,\sigma}), \tag{2}$$

where $a_{i,\sigma}$ denotes the annihilation operator at site i with spin σ and $b_{i,\sigma}$ denotes the annihilation operator in the corresponding mode in the second copy of the system[5].

[5] To strictly realize (2) one needs additional phase shifts. They can be obtained by shifting the energies of the two copies relative to each other in an additional step, e.g. using a superlattice. However, due to the particle number superselection rule (see appendix A) these phase shifts do not affect the final measurement result, and are not necessary for the present protocol.

Table 1. Rules determining the measurement outcome for fermions. For a derivation see section 2.2.

$N_{\mathrm{tot}}^{\mathcal{R}}$	$N_{\mathrm{tot}}^{\mathcal{R}}/2$	$N_1^{\mathcal{R}}$	Result for $V_2^{\mathcal{R}}$
Even	Even	Even	1
Even	Even	Odd	−1
Even	Odd	Even	−1
Even	Odd	Odd	1
Odd	–	–	0

(iii) Finally we measure site- and spin-resolved the occupation numbers using a quantum gas microscope [9, 10]. We denote the measurement results in copy one by $n_{i,\sigma}^{(1)}$ and in copy two by $n_{i,\sigma}^{(2)}$. In the case of fermions this number is either zero or one due to the Pauli principle, but also for bosons it suffices to determine the parity of the occupation number.
The difference between bosons and fermions consists of how the measured occupation numbers relate to the measured value of the operators $V_2^{\mathcal{R}}$.

Bosons. If one finds an even (odd) number of bosons on the modes belonging to $\mathcal{R}$ of copy one, then the measurement outcome for $V_2^{\mathcal{R}}$ is plus (minus) one [11].

Fermions. For fermions the measurement outcome of the operator $V_2^{\mathcal{R}}$ depends on the total number of fermions in both copies of the modes belonging to $\mathcal{R}$, which we denote by $N_{\mathrm{tot}}^{\mathcal{R}} = \sum_{(i,\sigma)\in\mathcal{R}} n_{i,\sigma}^{(1)} + n_{i,\sigma}^{(2)}$, and on the number of atoms on copy one of the modes belonging to $\mathcal{R}$, denoted by $N_1^{\mathcal{R}} = \sum_{(i,\sigma)\in\mathcal{R}} n_{i,\sigma}^{(1)}$. The corresponding measurement result for $V_2^{\mathcal{R}}$ can be read off from table 1.

To determine the expectation value of $V_2^{\mathcal{R}}$, and thus the purity of the corresponding reduced density operator, one has to repeat the whole measurement procedure and average over the outcomes. Since all the swap operators for different subsets $\mathcal{R}$ commute ($[V_2^{\mathcal{R}}, V_2^{\mathcal{R}'}] = 0$), it is in principle possible to measure all of them at once. In fact in each single run one obtains a measurement result for all possible subsets.

2.2. *Justification of the measurement protocol*

Here we show that the above protocol implements a measurement of the swap operator and thus the Renyi entropy. We give the proof for V_2 and at the end comment on $V_2^{\mathcal{R}}$.

As we noted above, the swap operator V_2 acts on the Fock states according to $V_2|\mathbf{n}, \mathbf{m}\rangle = |\mathbf{m}, \mathbf{n}\rangle$. In the bosonic case it is simply given by the operator which interchanges $a_i^\dagger \leftrightarrow b_i^\dagger$, since the order of the creation operators does not matter for bosons. However for fermions applying V_2 is *not* equivalent to exchanging $a_i^\dagger \leftrightarrow b_i^\dagger$, since such an operation performs the mapping $|\mathbf{n}, \mathbf{m}\rangle \to (-1)^{\sum_{i,j} n_i m_j} |\mathbf{m}, \mathbf{n}\rangle$.

From the Fock-basis one can easily construct the eigenbasis of V_2. The eigenspace with eigenvalue +1 is spanned by vectors $|\psi_{\mathbf{n},\mathbf{m}}^+\rangle$ which are of the form $|\psi_{\mathbf{n},\mathbf{n}}^+\rangle = |\mathbf{n}, \mathbf{n}\rangle$, and $|\psi_{\mathbf{n},\mathbf{m}}^+\rangle = \frac{1}{\sqrt{2}}(|\mathbf{n}, \mathbf{m}\rangle + |\mathbf{m}, \mathbf{n}\rangle)$ for $\mathbf{n} \neq \mathbf{m}$. The eigenspace with eigenvalue −1 is spanned by the vectors

$|\psi^-_{\mathbf{n},\mathbf{m}}\rangle = \frac{1}{\sqrt{2}}(|\mathbf{n},\mathbf{m}\rangle - |\mathbf{m},\mathbf{n}\rangle)$. Under the beam-splitter operation equation (2) the eigenstates of V_2 transform into a superposition of states in the occupation number basis according to

$$U_2|\psi^\pm_{\mathbf{n},\mathbf{m}}\rangle = \sum_{\mathbf{k}} c^\pm_{\mathbf{k};\mathbf{n},\mathbf{m}}|\mathbf{k},\mathbf{n}+\mathbf{m}-\mathbf{k}\rangle. \tag{3}$$

The coefficients $c^\pm_{\mathbf{k};\mathbf{n},\mathbf{m}}$ depend on whether we are considering bosons or fermions. We discuss the two cases separately.

Bosons. The coefficients in equation (3) are given by

$$c^\pm_{\mathbf{k};\mathbf{n},\mathbf{m}} = \left(1 \pm (-1)^{\sum_j k_j}\right) d_{\mathbf{k};\mathbf{n},\mathbf{m}}, \tag{4}$$

where $d_{\mathbf{k};\mathbf{n},\mathbf{m}}$ is a numerical factor which is irrelevant for the following discussion. From equations (3) and (4) we see that the beam splitter operation transforms the symmetric states $|\psi^+_{\mathbf{n},\mathbf{m}}\rangle$, that is the eigenspace with eigenvalue +1 into the space with an even number of atoms in the first copy, since all coefficients for states with an odd number of atoms in copy one, $\sum_i k_i$, vanish after the application of the beam splitter. Similarly the eigenspace with eigenvalue -1 is transformed into the space with an odd number of atoms in the first copy.

Fermions. We find for fermions

$$c^\pm_{\mathbf{k};\mathbf{n},\mathbf{m}} = \left(1 \pm (-1)^{\sum_j k_j + \sum_{i,j} n_i m_j}\right) e_{\mathbf{k};\mathbf{n},\mathbf{m}}, \tag{5}$$

where $e_{\mathbf{k};\mathbf{n},\mathbf{m}}$, as for bosons, is a numerical factor which is irrelevant for our purpose. The main difference to the bosonic case is the dependence on the parity of the term $\sum_{i,j} n_i m_j$ in the exponent. If this term is even, the situation is the same as for bosons, and the symmetric states are mapped onto states with an even number of particles in copy one, while antisymmetric states are mapped onto states where this number is odd. However if $\sum_{i,j} n_i m_j$ is odd, the situation is reversed. Unfortunately, there is no way of determining the parity of $\sum_{i,j} n_i m_j$ after the beam splitter operation has been applied. One only has access to the values of k_i and $n_i + m_i$, that is the number of particles in the modes of copy one after the beam splitter, and the total number of atoms in both copies of each mode (which is the same before and after the beam splitter operation). However, we will show in the following that this is sufficient information to proceed. The basic idea is the following.

(i) Firstly, consider only the eigenstates $|\psi^\pm_{\mathbf{n},\mathbf{m}}\rangle$ with $\sum_i n_i = \sum_i m_i \equiv N$, that is with an equal number of atoms in the two systems (before the beam splitter operation is applied). For these eigenstates the parity of $\sum_{i,j} n_i m_j = N^2$ can be determined from the knowledge of the total number of atoms $N_{\text{tot}} = 2N$, which can be accessed from the occupation number measurement in the final step of our protocol. If N is even, then N^2 is even as well, and as in the bosonic case, the (anti-) symmetric states are mapped onto the space with (odd) even number of particles in copy one. On the other hand, if N is odd, then also N^2 is odd, and the situation is reversed, the (anti-) symmetric states are mapped onto the space with (even) odd number of particles in copy one. This is reflected in the rules presented in table 1.

(ii) Secondly, consider only the eigenstates $|\psi^\pm_{\mathbf{n},\mathbf{m}}\rangle$ with $\sum_i n_i \neq \sum_i m_i$. Then the total number of fermions N_{tot} is not enough to determine the parity of $\sum_{i,j} n_i m_j$. Thus, when assigning a measurement outcome according to table 1, there are some pairs $(\mathbf{n},\mathbf{m})$ where one incorrectly assigns a measurement result of +1 to the state $|\psi^-_{\mathbf{n},\mathbf{m}}\rangle$ and a value of -1 to the corresponding state $|\psi^+_{\mathbf{n},\mathbf{m}}\rangle$. However, for product states constrained by a particle number superselection rule [41] it is readily shown (see appendix A) that the probability of finding the system in the symmetric state $|\psi^+_{\mathbf{n},\mathbf{m}}\rangle$ is the same as the probability of finding it in

the corresponding antisymmetric state $|\psi^-_{\mathbf{n},\mathbf{m}}\rangle$, if $\sum_i n_i \neq \sum_i m_i$. Therefore these instances average to zero and the error is irrelevant for the average value. Furthermore, if the total number of atoms N_{tot} is odd, then one can be sure that $\sum_i n_i \neq \sum_i m_i$, and assign a measurement value of zero right away, as suggested in table 1. A more formal and detailed proof of these points can be found in appendix A. In contrast to the bosonic case [11], the above arguments cannot be generalized in a straightforward way to higher order Renyi entropies for fermions.

If one is interested in the purity of the reduced density operator of a subset of modes $\mathcal{R}$, that is in the measurement of $V_2^{\mathcal{R}}$, the discussion is completely analogous. Note that, since the beam splitter is unitary and the beam splitting operations for different modes commute, it is irrelevant whether or not one performs the beam splitter operation also on modes not belonging to $\mathcal{R}$. Thus in practice one can perform always the full beam splitter U_2 on each pair of modes, and determine the number of atoms and the corresponding measurement result for $V_2^{\mathcal{R}}$ in each subdivision $\mathcal{R}$ simultaneously.

2.3. Limitations and effect of errors

The main limitation of the proposed measurement scheme is that the number of single measurements necessary to determine the entropy with a certain statistical accuracy can become large. This number can be estimated as follows. Each single measurement gives, according to table 1 either ± 1 or 0. Their mean value determines $\langle V_2^{\mathcal{R}}\rangle = \mathrm{Tr}\{\rho_{\mathcal{R}}^2\}$. The variance of the measurement outcomes can be expressed as $(\Delta V_2^{\mathcal{R}})^2 = \langle P_{\mathrm{even}}\rangle - \langle V_2^{\mathcal{R}}\rangle^2$, where P_{even} is the projector on the sector with even total number of particles in the two copies. It is easily shown for product states of two copies, both constrained by a particle number superselection rule, that $1/2 \leqslant \langle P_{\mathrm{even}}\rangle \leqslant 1$. To determine the expectation value of $V_2^{\mathcal{R}}$ and thus the purity with a certain statistical accuracy σ_V, one needs a number of measurements $\#_V$ that is given by $\#_V \sigma_V^2 = \langle P_{\mathrm{even}}\rangle / \langle V_2^{\mathcal{R}}\rangle^2 - 1$. For highly mixed states this number diverges as $\#_V \sigma_V^2 \sim 1/\mathrm{Tr}\{\rho^2\}$. This results in an exponential scaling of the required number of measurements with the Renyi entropy. To determine the entropy with a relative statistical uncertainty of σ_S one needs $\#_S$ measurements with $\#_S \sigma_S^2 = \frac{1}{S_2^2}(\langle P_{\mathrm{even}}\rangle \mathrm{e}^{2S_2} - 1) \sim \mathrm{e}^{2S_2 - 2\log S_2}$. We note that all known schemes to measure entropy based on multiple copies [11, 36, 42] suffer from this limitation.

Since the (parity of the) number of atoms on each site enters crucially in the measurement result, errors in the measurement of this numbers are a major error source in an experiment. Their effect is most easily outlined in the measurement scheme for bosons, but the discussion can be carried out analogously for fermions. In an ideal experimental implementation the system state determines the probability $p_\pm$ of finding an eigenvalue plus or minus one, such that $\langle V_2\rangle = p_+ - p_-$. Suppose that with a probability ϵ the quantum gas microscope incorrectly measures an even (odd) number of particles on a certain site, when there is actually an odd (even) number of atoms. Assuming that such errors occur in an uncorrelated fashion and with the same probability on the M sites that are measured, the experimentally determined expectation value $\langle V_2\rangle_\epsilon$ is reduced compared to the actual one by $\langle V_2\rangle_\epsilon = \langle V_2\rangle(1-2\epsilon)^M$. Thus the measured entropy $S_{2,\epsilon}(\rho)$ is just the sum of the actual entropy of the system $S_2(\rho)$ and a contribution from the quantum gas microscope $S_{\mathrm{microscope}} = -M\log(1-2\epsilon)$, where the contribution of the quantum gas microscope is extensive in the size of the measured (sub)system. Thus, the measured purity (entropy) is always smaller (larger) than the actual one.

A general assumption [43] underlying the protocol is the preparation of two perfect copies $\rho \otimes \rho$. Even though our protocol does not provide a direct means to check this assumption, it can strengthen it *a posteriori*, e.g. if the two copies are close to a pure state. Then the measured expectation value is one if the state in both copies is the same. Also, one can relax the assumption of having completely uncorrelated copies and allow for classical correlations between them, such that the total density operator is of the form $\rho_{\text{tot}} = \sum_i p_i \rho_i \otimes \rho_i$, and still obtain useful information from the described measurement protocol as outlined in appendix B. On the other hand, one might be interested in the overlap of two states that are different from the outset. By preparing the two states in the form $\rho_1 \otimes \rho_2$, this protocol gives access to $\text{Tr}\{\rho_1 \rho_2\} = \text{Tr}\{V_2 \rho_1 \otimes \rho_2\}$.

3. Renyi entropies of a fermionic Hubbard chain

The protocol to measure Renyi entropies for fermionic systems described in the previous section provides a novel tool to access in experiments fundamental properties of many-body systems related to entanglement and thermal entropy. One of the important results quantum information theory has brought to the field of quantum many-body systems is the finding that ground states of local Hamiltonians typically exhibit an entropic area law $S \sim \alpha \partial A$, where ∂A denotes the perimeter of the boundary delimiting the two complementary subregions A and B [44]. In the particular case of 1D critical systems admitting a CFT description, the area-law picks up an (additive) logarithmic correction, whose prefactor solely depends on the central charge c of the CFT. These are very important theoretical results underlying the success of matrix- and tensor network based numerical and conceptional methods, and have furthermore deep connections to quantum field theory, string theory and black hole physics. It is therefore highly desirable to test these theoretical predictions in actual experiments, enabled through the experimental protocols introduced in previous [11, 36, 42] and the present work.

In this section we illustrate this for the example of the Fermi–Hubbard model in one dimension, as it is the simplest model of interacting fermions that can be realized with cold fermionic atoms in an optical lattice. In terms of creation ($a^\dagger_{i,\sigma}$), annihilation ($a_{i,\sigma}$) and counting operators ($n_{i,\sigma} = a^\dagger_{i,\sigma} a_{i,\sigma}$) the Fermi–Hubbard Hamiltonian for a 1D lattice with L sites is given by

$$H = -t_{\text{F}} \sum_{\sigma=\uparrow,\downarrow} \sum_{i=1}^{L-1} (a^\dagger_{i,\sigma} a_{i+1,\sigma} + \text{h.c.}) + U \sum_{i=1}^{L} n_{i,\uparrow} n_{i,\downarrow}, \tag{6}$$

where t_{F} denotes the hopping amplitude between neighboring sites and U the onsite interaction energy. The model is exactly solvable via the Bethe ansatz [45, 46] and the phase diagram exhibits a metallic two-channel Luttinger liquid ground state at generic fillings for all interactions $U \geqslant 0$ [46, 47]. At half filling and $U > 0$ the charge degrees of freedom are gapped and a Mott insulator appears.

Here, we use a generalized directed loop algorithm within the stochastic series expansion framework [48–50] to access the thermal Renyi entropies following a measurement scheme based on the dynamic update of the world line topologies presented in [21]. Large blocks are built up consecutively using the *increment trick* [51] that allows for an efficient update in replica space.

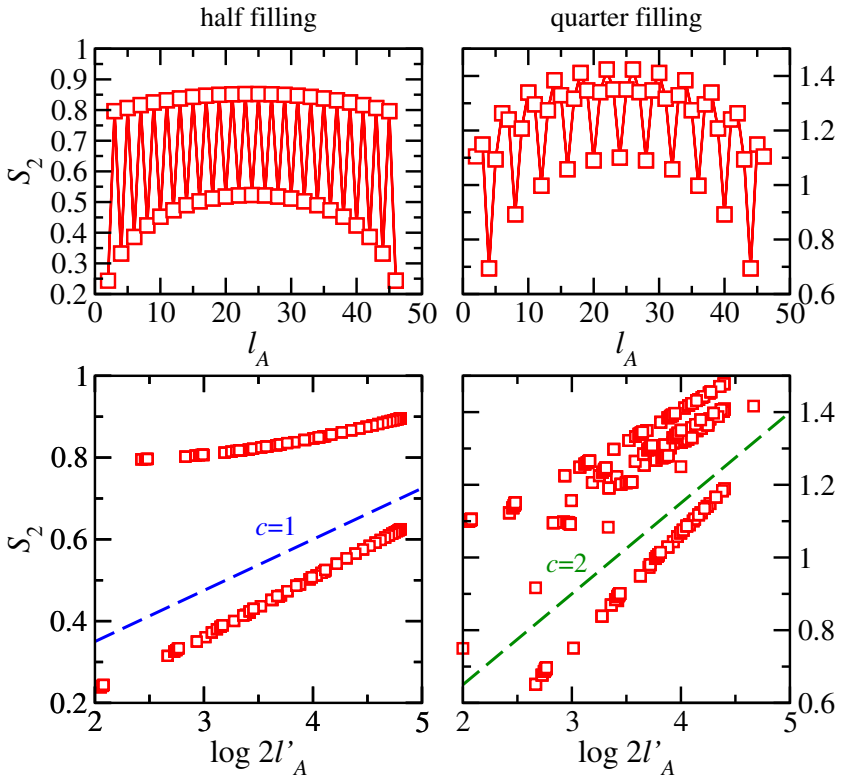

Figure 2. The upper left (right) panel shows the second Renyi entropy S_2 for the half-filled (quarter-filled) Hubbard model as a function of the chord distance l'_A for $L = 48$ and $U/t_F = 8$ obtained using DMRG. The lower panel displays the same entropy data as a function of $\log l'_A$, where l'_A is the chord length of block A. Here, we show DMRG data for systems up to $L = 96$. The slope of S_2 is given by $c/8$ (see equation (7)) and the blue and green lines are guides to the eye corresponding to $c = 1$ and 2 respectively.

In the following we quantify the ground-state entanglement as well as the thermal Renyi entropy that one would obtain with the proposed protocol for realistic experimental system sizes. We show to what extent quantum entanglement can be accessed through a measurement of S_2 for system sizes and temperatures available in an experiment. A systematic study of the crossover between entanglement and thermal entropy is presented in [33].

3.1. Zero temperature

Let us start by looking at the Hubbard chain at zero temperature. Figure 2 shows the $n = 2$ Renyi profiles for bipartitions $A \cup B$ with block sizes l_A obtained using DMRG for chains with $L = 48$ sites, both for half ($n_\uparrow = n_\downarrow = 1/2$) and quarter filling ($n_\uparrow = n_\downarrow = 1/4$). A prominent feature of the Renyi profiles for finite system sizes is that they exhibit characteristic oscillation associated with the Fermi-momentum k_F, giving rise to two (four) branches at half (quarter) filling. Further, one clearly identifies the envelope carrying the logarithmic corrections to the area law.

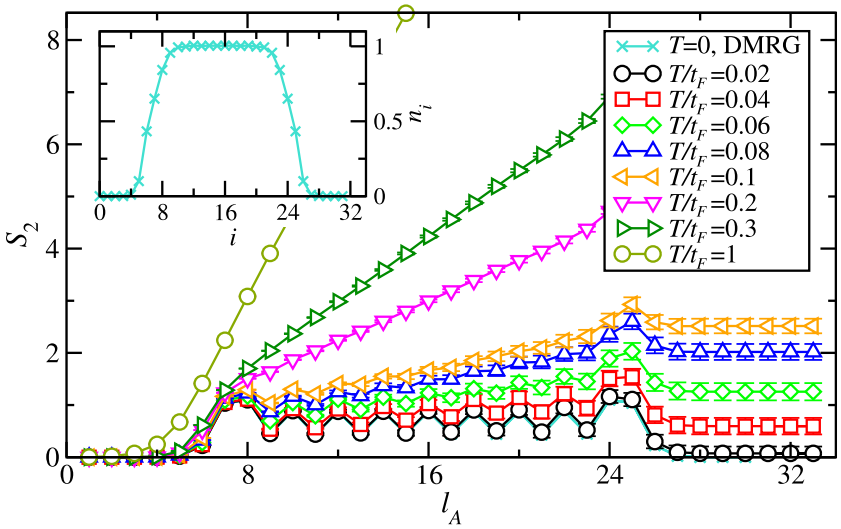

Figure 3. Renyi profile for a Hubbard chain in the presence of a trapping potential with $V(i) = (i - L/2)^2/20 - 6$ and $U/t_F = 6$. The green crosses correspond the ground-state of the system obtained from DMRG with 18 particles whereas the finite-temperature results are obtained from QMC using grand-canonical simulations with an average particle number coinciding to the $T = 0$ DMRG calculations. A density profile for different temperatures is shown in the inset.

These features are well understood via the underlying CFT [52–55], from which the Renyi profiles are obtained to be

$$S_n(A) = \frac{c}{12}\left(1 + \frac{1}{n}\right)\log 2\, l'_A + S_n^{\mathrm{corr}}(l'_A) + \text{const.}, \tag{7}$$

where $l'_A = L/\pi \sin(\pi l_A/L)$ is the chord distance. The first term is the leading contribution and describes the logarithmic increase of the entropy with block size. It is directly proportional to the central charge c and distinguishes between the metal ($c = 2$) and the Mott insulating state ($c = 1$) having two respectively one gapless channels. By measuring the Renyi profiles with the previously introduced protocol it is in principle possible to determine this pre-factor and to extract the central charge c in an experiment. This is conveniently done by plotting S_2 as a function of $\log(2l'_A)$, as shown in figure 2. This way, S_2 approaches a straight line with slope $c/12(1 + 1/n)$ for large block and system sizes. One can see from figure 2 that the data for the half filled Hubbard Model at $U/t_F = 8$ is consistent with a central charge of $c = 1$, as the two branches of the Renyi entropy approach the corresponding asymptotic line from above and below whereas the quarter filled chain exhibits $c = 2$.

3.2. Finite temperature and trap

A measurement of the Renyi Profile as proposed in section 2 will necessarily be performed at finite temperature. Then, the Renyi entropy will not only pick up quantum entanglement but also thermal contributions to the entropy. Since the thermal entropy is an extensive quantity, one expects a crossover from the area-law to a volume law. This is shown in figure 3,

where we plot finite-temperature QMC results for $U/t_F = 6$. To make a closer connection to the experimental situation, we include a harmonic trapping potential, $H_{trap} = \sum_i V_i n_i$, with $V(i) = (i - L/2)^2/20 - 6$. Filling the trap with 18 particles, at zero temperature a Mott insulator extends over about eight lattices sites and the density drops to zero in the wings quite rapidly (see the density profile in the inset of figure 3). In the center of the trap at $T = 0$, where the Mott phase proliferates, the Renyi profile shows the characteristic $2k_F$ oscillations. The metallic wings that appear due to the presence of the harmonic trap, are also clearly visible in the Renyi profile in figure 3.

When the temperature is increased above the finite size gap, the entropy S_2 picks up a linear contribution (see figure 3). Thus, the S_2 profile is no longer symmetric with respect to the center of the system and the purity of the whole system decreases as $S_2(L)$ increases. In addition the amplitude of the parity induced oscillations is suppressed as the temperature is increased. One can see that for temperature $T/t_F \gtrsim 0.1$, the entropy is already dominated by a linear increase of the thermal entropy and S_2 loses its parity effects.

The ability to measure Renyi profiles also allows access to other quantities that provide further insight into the entanglement and correlation properties of the system. For instance, the mutual information between two (possibly disjoint) blocks A and B and is given in terms of the Renyi entropies as

$$I_2(A|B) = S_2(A) + S_2(B) - S_2(A \cup B). \tag{8}$$

This measure is particularly useful when dealing with mixed states as it does not pick up an extensive contribution from the thermal entropy—it obeys an area law [14, 56, 57] even at finite-T—but is sensitive toward correlations between the two subblocks [58]. For a detailed discussion of the mutual information in the Hubbard chain we refer to [33].

3.3. Limitations

As pointed out in section 2.3, the ability to determine these entropy profiles using the protocol proposed in this work is fundamentally limited by an exponential growth with entropy of the number of single measurements required to obtain a certain statistical accuracy σ_S (see figure 4). To give numbers, for example 10^5 single measurements are needed to determine Renyi entropies up to $S_2 \sim 5$ with a relative statistical error of $\sigma_S \sim 0.1$. For 1D systems, at temperatures below the finite size gap this is not a severe restriction as the entropy obeys a area law with at most logarithmic corrections. For example in the previous subsection we showed that in the 1D Hubbard model, at temperatures below the finite size gap the entropies are typically of the order one. This values can be resolved with just $\sim 10/\sigma_S^2$ single measurements. Above the finite size gap however the number of measurements sets the limit in terms of temperatures and system sizes, as the entropy becomes extensive in the system size and increases with temperature.

To quantify this, figure 4 shows the Renyi entropy $S_2(L)$ of a full (homogeneous) Hubbard chain at quarter filling and $U/t_F = 4$ as a function of system size L (open boundary conditions) and temperature T, as well as the number of measurements, $\#_S$, required to resolve a certain value of S_2 with a statistical relative error, σ_S, using the above proposed protocol. This clearly shows that experimentally relevant situations, e.g. $T/t_F \sim 0.2$, $L \sim 30$ can be explored with a moderate number $\#_S \sigma_S^2 \lesssim 10^3$ of single measurements.

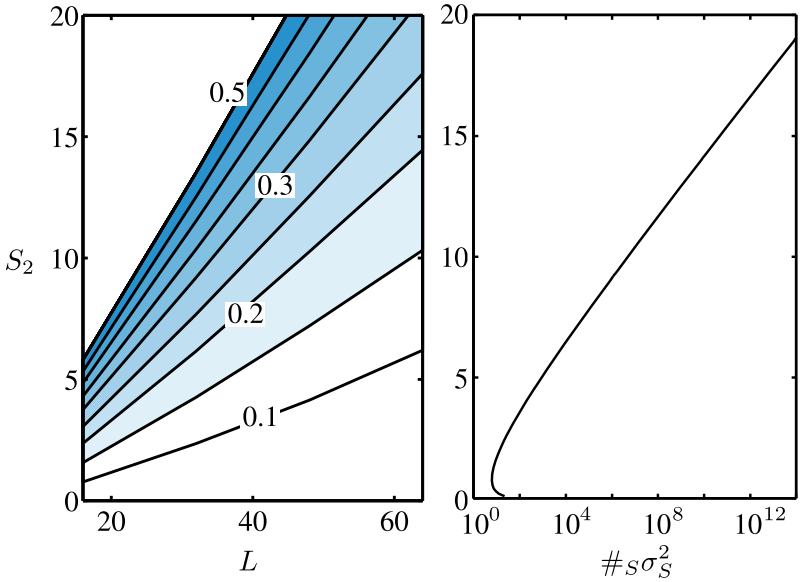

Figure 4. (left) Renyi entropy of the whole chain, $S_2(L)$ at quarter filling and $U/t_F = 4$, for different system sizes L at different temperatures T. The contour lines denote constant temperature $T/t_F = 0.1, 0.15, \ldots, 0.5$. (right) Number of measurements, $\#_S$, required for a measurement of S_2 with a statistical relative error σ_S, using our protocol.

4. Discussion

To summarize, we have presented a method to determine the order two Renyi entropy for bosons and fermions in an optical lattice. The scheme is based on the possibility of preparing two identical copies of a quantum state in an optical lattice, coupling the two copies via a superlattice, and site-(and spin-)resolved measurement of the occupation number (modulo two). The combination of these tools, which are available in current experiments, allows one to directly determine the entropy of a many-body quantum state, and may be seen as a thermometer for states near the absolute ground state. On the other hand, for pure states this opens the possibility to study entanglement as quantified by the entropy of a subsystem. Possible applications include test area laws for the scaling of entanglement entropy in ground states, and monitoring entanglement in time-dependent systems. Using QMC-techniques we analyzed the possibility to test area laws and their corrections in a finite size system at finite temperatures typically present in current experiments.

Acknowledgments

We thank I Bloch, M Greiner, C Groß and M Zwierlein, for helpful and motivating discussions. Work in Innsbruck is supported in part by the EU project AQUTE, the Austrian Science Fund (FWF) through SFB FOQUS and the Austrian Ministry of Science BMWF as part of the UniInfrastrukturprogramm of the Research Platform Scientific Computing at the University of Innsbruck. Work in Pittsburgh is supported by a grant from the US Army Research Office with funding from the DARPA OLE program and by NSF grant PHY-1148957.

Appendix A. Details on the proof of the measurement protocol

Here we elaborate more formally on some points of the proof presented in section 2.2 for fermions. First, note that a pure state (in one copy) with N fermions (constrained by the particle number superselection rule) always has the form

$$|\psi\rangle = \sum_{\substack{\mathbf{n} \\ \sum_i n_i = N}} \psi_{\mathbf{n}} |\mathbf{n}\rangle, \tag{A.1}$$

where N is the total number of atoms. A general state is a mixture of such states (with possibly different total number of fermions)

$$\rho = \sum_N \sum_{\substack{\mathbf{n},\mathbf{n}' \\ \sum_i n_i = N \\ \sum_i n'_i = N}} \rho^{(N)}_{\mathbf{n},\mathbf{n}'} |\mathbf{n}\rangle\langle\mathbf{n}'|. \tag{A.2}$$

Thus, a general *product* state in the two systems has the form

$$\rho \otimes \tilde{\rho} = \sum_{N,M} \sum_{\substack{\mathbf{n},\mathbf{n}' \\ \sum_i n_i = N \\ \sum_i n'_i = N}} \sum_{\substack{\mathbf{m},\mathbf{m}' \\ \sum_i m_i = M \\ \sum_i m'_i = M}} \rho^{(N)}_{\mathbf{n},\mathbf{n}'} \tilde{\rho}^{(M)}_{\mathbf{m},\mathbf{m}'} |\mathbf{n},\mathbf{m}\rangle\langle\mathbf{n}',\mathbf{m}'|. \tag{A.3}$$

They have the crucial property that for $\sum_i n_i \neq \sum_i m_i$ one has

$$\langle\psi^+_{\mathbf{n},\mathbf{m}}|\rho \otimes \tilde{\rho}|\psi^+_{\mathbf{n},\mathbf{m}}\rangle = \langle\psi^-_{\mathbf{n},\mathbf{m}}|\rho \otimes \tilde{\rho}|\psi^-_{\mathbf{n},\mathbf{m}}\rangle, \tag{A.4}$$

as one can easily show using the definition of the eigenstates (see section 2.2) and equation (A.3). This property is used to allow for errors in the assignments of the measured eigenvalue, that do not alter the average value. An alternative way of thinking about this is the following. We want to determine the purity of ρ via the expectation value $\mathrm{Tr}\{\rho^2\} = \mathrm{Tr}\{V_2 \rho \otimes \rho\}$. However V_2 is not the only operator whose expectation value in the state $\rho \otimes \rho$ is equal to $\mathrm{Tr}\{\rho^2\}$. Below we will introduce a whole family of operators $V_2^{(f)}$ (depending on some function f), which share this property. We define

$$P_\pm(\mathbf{n},\mathbf{m}) = \tfrac{1}{2}(|\mathbf{n},\mathbf{m}\rangle \pm |\mathbf{m},\mathbf{n}\rangle)(\langle\mathbf{n},\mathbf{m}| \pm \langle\mathbf{m},\mathbf{n}|), \tag{A.5}$$

and further $Q(\mathbf{n},\mathbf{m}) = \frac{1}{2}(P_+(\mathbf{n},\mathbf{m}) - P_-(\mathbf{n},\mathbf{m}))$, such that we can write $V_2 = \sum_{\mathbf{n},\mathbf{m}} Q(\mathbf{n},\mathbf{m})$. The factor $1/2$ in the definition of Q is to correct for double-counting. We can divide the eigenstates of V_2 in two classes, those with $\sum_i n_i = \sum_i m_i$ and the others, leading to the representation

$$V_2 = \sum_{\substack{\mathbf{n},\mathbf{m} \\ \sum_i n_i = \sum_i m_i}} Q(\mathbf{n},\mathbf{m}) + \sum_{\substack{\mathbf{n},\mathbf{m} \\ \sum_i n_i \neq \sum_i m_i}} Q(\mathbf{n},\mathbf{m}). \tag{A.6}$$

Note that due to equation (A.4), the expectation value of each term in the second sum is identically zero for states of the form equation (A.3). Therefore, the expectation value of the operator V_2 is the same as the one of $V_2^{(f)}$ defined as

$$V_2^{(f)} = \sum_{\substack{\mathbf{n},\mathbf{m} \\ \sum_i n_i = \sum_i m_i}} Q(\mathbf{n},\mathbf{m}) + \sum_{\substack{\mathbf{n},\mathbf{m} \\ \sum_i n_i \neq \sum_i m_i}} f(\mathbf{n},\mathbf{m}) Q(\mathbf{n},\mathbf{m}), \tag{A.7}$$

where $f(\mathbf{n}, \mathbf{m})$ is an arbitrary (real-valued) function. In particular we can choose

$$f(\mathbf{n}, \mathbf{m}) = \begin{cases} 0, & s(\mathbf{n}+\mathbf{m}) = 1, \\ 1, & s(\mathbf{n}) = s(\mathbf{m}) = s((\mathbf{n}+\mathbf{m})/2), \\ -1, & s(\mathbf{n}) = s(\mathbf{m}) \neq s((\mathbf{n}+\mathbf{m})/2), \end{cases} \tag{A.8}$$

where we use the notation $s(\mathbf{x}) = \sum_i x_i \bmod 2$. The eigenstates of $V_2^{(f)}$ are the same as those of V_2, but they have different eigenvalues. The advantage of choosing f in the above form is that the eigenvalue of $V_2^{(f)}$ can be determined from the total number of atoms and the number of atoms in copy one after the beam splitter, as presented in table 1. This can easily be checked by explicitly looking at the transformation of all the different classes of eigenstates of $V_2^{(f)}$ under the beamsplitter.

Appendix B. Mixtures of copies

As pointed out in [36] the expectation value of the operator V_2 in the state $\rho_{\text{tot}} = \rho \otimes \rho$ is given by $\text{Tr}\{\rho^2\}$. The assumption of having two completely uncorrelated copies of the form $\rho_{\text{tot}} = \rho \otimes \rho$, although being difficult to validate [43] experimentally, is a natural one for such systems in optical lattices, where the two copies can be decoupled by a high potential barrier. However, correlated errors, such as for example global fluctuations in the intensities of the laser beam that generates the lattice [59], affect the two copies in the same way and lead to correlations between the copies. Such identical, but correlated errors in general lead to a state which is a mixture of different products of the same state, that is $\rho_{\text{tot}} = \sum_i p_i \rho_i \otimes \rho_i$ with $\sum_i p_i = 1$ and $p_i \geqslant 0$. In the following we show that even in this situation the measurement of the operator V_2 provides useful information about the entropy in the sense that it provides bounds on the purity of the reduced system of one of the two 'copies', that is of the state $\rho \equiv \text{Tr}_{\text{copy2}}\{\rho_{\text{tot}}\} = \sum_i p_i \rho_i$. To this end we show that

$$\tfrac{1}{2}\text{Tr}\{V_2 \rho_{\text{tot}}\} \leqslant \text{Tr}\{\rho^2\} \leqslant \text{Tr}\{V_2 \rho_{\text{tot}}\}. \tag{B.1}$$

We first show the upper bound. Consider the function

$$F(\{p_i\}) \equiv \text{Tr}\{\rho^2\} - \text{Tr}\{V_2 \rho_{\text{tot}}\} = \sum_{i,j} p_i p_j \,\text{Tr}\{\rho_i \rho_j\} - \sum_i p_i \,\text{Tr}\{\rho_i^2\}, \tag{B.2}$$

defined in the polytope spanned by the p_i with $\sum_i p_i = 1$ and $p_i \geqslant 0$. Note that this function is zero at the corners of this polytope given by $p_i = \delta_{i,j}$. Further, the Hessian matrix of F is constant and given by $H_{i,j} \equiv \frac{\mathrm{d}^2 F}{\mathrm{d}p_i \mathrm{d}p_j} = 2\,\text{Tr}\{\rho_i \rho_j\}$. This is a Gramian matrix and thus positive semidefinite. Thus the function F is convex everywhere and its value on the (convex) polytope defined by $\sum_i p_i = 1$ and $p_i \geqslant 0$ is smaller than its value at the corners. This proves the upper bound. To prove the lower bound we calculate the (unique) global minimum of F. It is assumed at the position that satisfies $\mathrm{d}F/\mathrm{d}p_i \equiv \sum_j 2 p_j \text{Tr}\{\rho_i \rho_j\} - \text{Tr}\{\rho_i^2\} = 0$. That is, at the minimum we find $\sum_j p_j \text{Tr}\{\rho_i \rho_j\} = \frac{1}{2}\text{Tr}\{\rho_i^2\}$. Using this in equation (B.2) we find that $F \geqslant -\frac{1}{2}\sum_i p_i \,\text{Tr}\{\rho_i^2\} = -\frac{1}{2}\text{Tr}\{V_2 \rho_{\text{tot}}\}$, and thus $\frac{1}{2}\text{Tr}\{V_2 \rho_{\text{tot}}\} \leqslant \text{Tr}\{\rho^2\}$. These inequalities trivially hold also for purities of subsystems of one of the two copies (with the corresponding swap-operators).

The inequalities equation (B.1) give bounds in terms of the expectation value of V_2 on arbitrary mixtures of copies. In the typical experiment situation one expects to be very close to

a simple product of two states with a small admixture of other copies, such that $p_0 = 1 - \epsilon$ with $\epsilon = \sum_{i\neq 0} p_i \ll 1$. Because the function $F(\{p_i\})$ is convex we can bound

$$F(\{p_i\}) \geqslant F(\{\delta_{i,0}\}) + \sum_i (p_i - \delta_{i,0}) \frac{\mathrm{d}F(\{p_i\})}{\mathrm{d}p_i}\Big|_{p_i=\delta_{i,0}} \tag{B.3}$$

$$= -\sum_{i\neq 0} p_i \,\mathrm{Tr}\{(\rho_i - \rho_0)^2\} \geq -2\sum_{i\neq 0} p_i \equiv -2\epsilon, \tag{B.4}$$

and thus one has $\mathrm{Tr}\{V_2\rho_{\mathrm{tot}}\} - 2\epsilon \leqslant \mathrm{Tr}\{\rho^2\} \leqslant \mathrm{Tr}\{V_2\rho_{\mathrm{tot}}\}$.

References

[1] Jaksch D and Zoller P 2005 *Ann. Phys.* **315** 52
[2] Bloch I and Zwerger W 2008 *Rev. Mod. Phys.* **80** 885
[3] Bloch I, Dalibard J and Nascimbène S 2012 *Nature Phys.* **8** 267
[4] Lewenstein M, Sanpera A and Ahufinger V 2012 *Ultracold Atoms in Optical Lattices: Simulating Quantum Many-Body Systems* (Oxford: Oxford University Press)
[5] Schneider U, Hackermuller L, Will S, Best T, Bloch I, Costi T A, Helmes R W, Rasch D and Rosch A 2008 *Science* **322** 1520
[6] Nascimbène S, Navon N, Jiang K J, Chevy F and Salomon C 2010 *Nature* **463** 1057
[7] Jördens R *et al* 2010 *Phys. Rev. Lett.* **104** 180401
[8] Zhang X, Hung C L, Tung S K and Chin C 2012 *Science* **335** 1070
[9] Bakr W S, Gillen J I, Peng A, Fölling S and Greiner M 2009 *Nature* **462** 74
[10] Sherson J F, Weitenberg C, Endres M, Cheneau M, Bloch I and Kuhr S 2010 *Nature* **467** 68
[11] Daley A, Pichler H, Schachenmayer J and Zoller P 2012 *Phys. Rev. Lett.* **109** 020505
[12] Schuch N, Wolf M M, Verstraete F and Cirac J I 2008 *Phys. Rev. Lett.* **100** 030504
[13] Calabrese P and Cardy J 2004 *J. Stat. Mech.* P06002
[14] Eisert J, Cramer M and Plenio M B 2010 *Rev. Mod. Phys.* **82** 277
[15] Fradkin E and Moore J E 2006 *Phys. Rev. Lett.* **97** 050404
[16] Ryu S and Takayanagi T 2006 *J. High Energy Phys.* JHEP08(2006)045
[17] Metlitski M A, Fuertes C A and Sachdev S 2009 *Phys. Rev.* B **80** 115122
[18] Tagliacozzo L, Evenbly G and Vidal G 2009 *Phys. Rev.* B **80** 235127
[19] Kallin A B, Hastings M B, Melko R G and Singh R R P 2011 *Phys. Rev.* B **84** 165134
[20] Metlitski M A and Grover T 2011 arXiv:1112.5166
[21] Humeniuk S and Roscilde T 2012 arXiv:1203.5752
[22] Ju H, Kallin A B, Fendley P, Hastings M B and Melko R G 2012 *Phys. Rev.* B **85** 165121
[23] Kitaev A and Preskill J 2006 *Phys. Rev. Lett.* **96** 110404
[24] Levin M and Wen X G 2006 *Phys. Rev. Lett.* **96** 110405
[25] Calabrese P and Cardy J 2005 *J. Stat. Mech.* P04010
[26] Läuchli A and Kollath C 2008 *J. Stat. Mech.* P05018
[27] Manmana S R, Wessel S, Noack R M and Muramatsu A 2009 *Phys. Rev.* B **79** 155104
[28] Cheneau M, Barmettler P, Poletti D, Endres H, Schauß P, Fukuhura T, Gross C, Bloch I, Kollath C and Kuhr S 2012 *Nature* **481** 484
[29] Kinoshita T, Wenger T and Weiss D S 2006 *Nature* **440** 900
[30] Hofferberth S, Lesanovsky I, Fischer B, Schumm T and Schmiedmayer J 2007 *Nature* **449** 324
[31] Rigol M, Dunjko V and Olshanii M 2008 *Nature* **452** 854
[32] Trotzky S, Chen Y A, Flesch A, McCulloch I P, Schollwock U, Eisert J and Bloch I 2012 *Nature Phys.* **8** 325
[33] Bonnes L, Pichler H and Läuchli A M 2013 arXiv:1304.5340

[34] Horodecki R, Horodecki M and Horodecki K 2009 *Rev. Mod. Phys.* **81** 865
[35] Mintert F and Buchleitner A 2007 *Phys. Rev. Lett.* **98** 140505
[36] Ekert A, Alves C, Oi D, Horodecki M, Horodecki P and Kwek L 2002 *Phys. Rev. Lett.* **88** 217901
[37] Simon J, Bakr W S, Ma R, Tai M E, Preiss P M and Greiner M 2011 *Nature* **472** 307
[38] Bolda E, Tiesinga E and Julienne P 2002 *Phys. Rev.* A **66** 013403
[39] Theis M, Thalhammer G, Winkler K, Hellwig M, Ruff G, Grimm R and Denschlag J H 2004 *Phys. Rev. Lett.* **93** 123001
[40] Fölling S, Trotzky S, Cheinet P, Feld M, Saers R, Widera A, Müller T and Bloch I 2007 *Nature* **448** 1029
[41] Schuch N, Verstraete F and Cirac J 2004 *Phys. Rev.* A **70** 042310
[42] Abanin D and Demler E 2012 *Phys. Rev. Lett.* **109** 020504
[43] van Enk S 2009 *Phys. Rev. Lett.* **102** 190503
[44] Eisert J and Prosen T 2010 arXiv:1012.5013
[45] Lieb E H and Wu F Y 1968 *Phys. Rev. Lett.* **20** 1445
[46] Essler F H L, Frahm H, Göhmann F, Klümper A and Korepin V E 2005 *The One-Dimensional Hubbard Model* (Cambridge: Cambridge University Press)
[47] Giamarchi T 2004 *Quantum Physics in One Dimension* (Oxford: Clarendon)
[48] Sandvik A W 1999 *Phys. Rev.* B **59** R14157
[49] Syljuåsen O F and Sandvik A W 2002 *Phys. Rev.* E **66** 046701
[50] Alet F, Wessel S and Troyer M 2005 *Phys. Rev.* E **71** 036706
[51] Hastings M B, González I, Kallin A B and Melko R G 2010 *Phys. Rev. Lett.* **104** 157201
[52] Calabrese P and Cardy J 2009 *J. Phys. A: Math. Theor.* **42** 504005
[53] Calabrese P, Campostrini M, Essler F and Nienhuis B 2010 *Phys. Rev. Lett.* **104** 095701
[54] Calabrese P and Essler F 2010 *J. Stat. Mech.* P08029
[55] Fagotti M and Calabrese P 2011 *J. Stat. Mech.* P01017
[56] Srednicki M 1993 *Phys. Rev. Lett.* **71** 666
[57] Amico L, Fazio R, Osterloh A and Vedral V 2008 *Rev. Mod. Phys.* **80** 517
[58] Wolf M M, Verstraete F, Hastings M B and Cirac J I 2008 *Phys. Rev. Lett.* **100** 070502
[59] Pichler H, Schachenmayer J, Simon J, Zoller P and Daley A 2012 *Phys. Rev.* A **86** 051605